

Multiple hyper-sonographic spots in basal cell carcinoma

Hisashi Uhara, MD, PhD; Koichi Hayashi, MD; Hiroshi Koga, MD;

Toshiaki Saida, MD, PhD

Corresponding author: Hisashi Uhara MD, PhD

Department of Dermatology, Shinshu University School of Medicine,

3-1-1 Asahi, Matsumoto 390-8621, Nagano, Japan

TEL: +81-263-37-2647, FAX: +81-263-37-2646

e-mail: uhara@hsp.md.shimshu-u.ac.jp

Author Contributions: Study concept and design: Uhara. Acquisition

of data: Uhara, Hayashi, and Koga. Analysis and interpretation of data:

Uhara, Hayashi, Koga, and Saida. Critical revision of the manuscript:

Uhara and Saida. Study supervision: Uhara and Saida.

Financial Disclosure: None.

Conflicts of Interest : None.

Word count: 1487

Short title: hyper-sonographic spots in BCC

ABSTRACT

BACKGROUND. High-frequency ultrasound is a useful method to obtain preoperative information regarding extension of basal cell carcinoma. However, its contribution to diagnosis is generally limited. Recently, we observed hyper-sonographic spots in some cases of basal cell carcinoma.

OBJECTIVE. The present study was performed to determine the diagnostic value of this finding in this type of tumor.

MATERIALS AND METHODS. We conducted a retrospective study of archived sonographic images with a 30 or 15 MHz scanner and histology specimens of a total of 85 lesions, consisting of 29 basal cell carcinomas and 56 melanomas.

RESULTS. The findings were classified into 4 patterns as follows: type A, multiple (over 5 spots/lesion) hyper-sonographic spots (14 cases, 48%); type B, sparse (3~5 spots/lesion) hyper-sonographic spots (7 cases, 24%); type C, multiple moderate-sonographic spots (3 cases, 10%); and type D, sparse moderate-sonographic spots (5 cases, 17%). Three of 56 melanoma lesions examined as controls showed the type D pattern, but none showed type A, B, or C patterns. Histopathologically, these hyper-sonographic spots in BCCs seemed to correspond to calcification, horn cysts, or clusters of apoptotic cells in the centers of nests of basal cell carcinoma.

CONCLUSION. Multiple hyper-sonographic spots might become a useful finding for differential diagnosis between basal cell carcinoma and melanoma.

INTRODUCTION

A diagnosis of basal cell carcinoma (BCC) is usually made based on macroscopic findings and confirmed by subsequent histopathological examination. Recently, epiluminescent technology, dermoscopy, has improved the accuracy of pre-operative diagnosis of BCC¹. Several characteristic findings of BCC have been reported, including arborizing vessels and large blue-grey ovoid nests. However, even using dermoscopy, we still encounter lesions that are difficult to diagnose as BCC.

Ultrasound sonography allows non-invasive assessment of skin tumors². To date, many studies have shown that this is a useful tool to evaluate the thickness and margins of skin tumors³⁻⁶. However, in general, the usefulness in determining diagnosis of skin tumors of ultrasound sonography seems to be limited^{7,8}.

Recently, using ultrasound sonography, we found that BCC showed multiple hyper-sonographic spots in the internal image. The present study was performed to determine whether this finding can aid in the diagnosis of BCC.

PATIENTS AND METHODS

Patients

The sonographic database of the Dermatology Clinic, Shinshu University Hospital, Matsumoto, Japan, for the years 1998 through 2005 was searched for diagnosis of BCC and melanoma primary lesions. The sonographic images of a total of 85 lesions, consisting of 29 BCCs and 56 melanomas, were available for examination. Sonographic evaluation was performed by a dermatologist (H.U.) without knowledge of the clinical or histopathological information.

Ultrasound equipment

The equipment used incorporates a single, mechanically activated 15- or 30-MHz transducer housed in a built-in water chamber (RION, Tokyo,

Japan). The number of A-lines is 100 in 15-MHz and 128 in 30-MHz. The maximum dimensions of a typical 2-dimension scan is 10 mm width x 10 mm depth in 15-MHz and 10 mm x 5 mm in 30-MHz. A thin, disposable plastic membrane covers the chamber window, and coupling with the surface of the tumor is achieved using gel for echography.

Histopathological study

To investigate the relationship between sonographic images and histopathological findings, we searched for calcification, horn cysts, or clusters of apoptotic cells in the tissue specimens.

RESULTS

All the BCC and melanoma lesions were well identified as solid hypo-sonographic areas under the entry echo line representing the gel-skin surface interface. All BCC lesions and 3 melanoma lesions showed some internal images. The images were clearer at 30-MHz than 15-MHz.

The internal images of BCC were classified into 4 patterns as follows: A, multiple (>5 spots/lesion) hyper-sonographic spots (14 lesions, 48%) (**Figure 1**); B, sparse (3~5 spots/lesions) hyper-sonographic spots (7 lesions, 24%); C, multiple moderate-sonographic spots (3 lesions, 10%); and D, sparse moderate-sonographic spots (5 lesions, 17%). Only 3 of 56 primary melanoma lesions showed the type D pattern and none of these lesions showed type A, B, or C patterns.

Heterogeneity in internal echo images seemed to be related to histopathological structures, including calcification, cornified cysts, clusters of parakeratotic cells, apoptotic cells, or necrosis in the tumor cell nests. The frequencies of histopathological structures observed in BCC showing each echographic pattern were as follows: calcification foci in 71% (11/14) of type A (**Figure 2**), 14% (1/7) of type B, 33% (1/3) of type C, and 20% (1/5) of type D. Cornified cysts or clusters of parakeratotic cells were observed in 79% of type A, 71% of type B, 100% of type C, and 90% of type D. Clusters of apoptotic cells or necrosis in the centers of the tumor nests were observed in 50% of type A, 29% of type B, and 0% of types C and D. The examined cases of BCC were consisting of 26 nodular and/or ulcerated type and 3 superficial

type, but no Morpheaform BCC. There were no differences among the histopathological subtypes of BCC except for superficial type, all of which showed the type D pattern. The tumor thickness of 3 melanomas showing type D was 1,06, 1.49 and 2.25 mm, respectively and there was no relationship between tumor thickness and internal sonographic images in melanoma.

Two types of hyper-sonographic spot were observed (**Figure 1**): large spots with indistinct margins with the appearance of cotton flowers, and small round spots (**Figure 3**). Numerous large foci of calcification were observed in the BCC lesions showing the former type. In contrast, in the lesions showing the latter type, calcification foci were small and sparse or rarely observed.

In the present series of BCC, two cases that were difficult to diagnose based on the results of dermoscopy showed the characteristic sonographic finding (**Figure 4**).

DISCUSSION

To date, many studies have shown that preoperative ultrasound sonography can provide useful information regarding tumor thickness or spread of cutaneous neoplasms²⁻⁶. Although there have been many attempts to identify sonographic patterns characteristic to different types of skin tumor, the significance of sonography in determining specific diagnosis is generally limited^{7,8}.

Previous studies showed that BCC has a hypoechoic structure with variable hyper-echogenicity⁸⁻¹². Harland *et al.* reported that variation of tumor echo pattern was determined by the distribution of collagen bundles and keratin-rich structures in the tumor mass. Interestingly, they showed a case of BCC in their review article, which had high echogenic spots correspond to keratin nests on histological section, some of which contained calcification. However, to date, this finding has not been focused. In the present study, multiple hyper-sonographic spots were observed in three quarters of BCC lesions but not in any melanoma lesions. Especially, multiple large spots with indistinct margins seemed to be characteristic of BCC.

Among the histopathological structures, it was likely that calcification most strongly affected the internal sonographic image of BCC. However,

calcification alone did not always influence the image. Numerous large calcification foci were observed in cases showing large and sonographic spots with indistinct margins. In contrast, calcification was sparsely observed or was lacking in cases showing small and round sonographic spots, as shown in Figure 3. These findings suggest that the small round hyper-sonographic spots could be formed not by only calcification but also by other histopathological structures, such as cornified cysts, clusters of parakeratotic or apoptotic cells, or necrosis.

Hyper-sonographic spots were not observed in type C or D, although histopathologically both types showed sparse calcification. As sonography has been used mainly for evaluation of the thickness and margins of tumors, we did not focus on the internal image. In addition, although sonographic images can be evaluated easily under real-time observation, it is frequently difficult to capture the sonographic spots on film when the spots are sparse. Thus, adequate images to allow capture of calcification may not be available in some cases. In addition, these reasons could be related to the disparity in the sonographic feature between the previous reports and our study.

Asian including Japanese often have pigmented BCCs, however, melanin could not influence the internal sonographic image, because multiple hyper-sonographic spots were observed in one case of non-pigmented BCC.

Our results suggest that hyper-sonographic spots might become a useful finding for differential diagnosis between BCC and melanoma. However, it is not yet possible to conclude whether tumors other than melanoma are sonographically distinguishable from BCC using this method. Walsh *et al.* reported that calcium deposits were observed histopathologically in 21% of BCC but were rarely seen in squamous cell carcinoma¹³. In addition, Bettencourt *et al.* reported that calcification was seen in 29% of trichoepitheliomas¹⁴. Calcification is not only observed in BCC but also in various pathological conditions, including tumors with follicular differentiation¹³. Therefore, further studies are required to clarify whether the presence of multiple hyper-sonographic spots is useful to distinguish BCC from other tumors, especially those with follicular differentiation.

Most cases of BCC can be diagnosed correctly by visual assessment,

including epiluminescent technology, dermoscopy¹. There are several well-known dermoscopic findings for diagnosis of BCC, such as arborizing vessels, large blue-grey ovoid nests, multiple blue-gray globules, maple leaf-like areas, and spoke-wheel areas. However, we still encounter BCC lesions that are difficult to diagnose even by dermoscopy. In our series, two cases of BCC showing the characteristic sonographic patterns did not exhibit dermoscopic findings characteristic of BCC. Thus, sonographic imaging could be useful as an additional non-invasive method for the diagnosis of BCC.

REFERENCES

1. Menzies SW, Westerhoff K, Ravinovitz H, Kopf AW, McCarthy WH, Katz B. Surface microscopy of pigmented basal cell carcinoma. *Arch Dermatol.* 2000; 136: 1012-1016
2. Schmid-Wendtner MH, Burgdorf W. Ultrasound Scanning in Dermatology. *Arch Dermatol.* 2005; 141: 217-224
3. Hoffman K, el Gammal S, Matthes U, Altmeyer P. Digital 20 MHz sonography of the skin in preoperative diagnosis. *Z Hautkr.* 1989; 64: 851-852, 855-858
4. Lassau N, Spatz A, Avril MF, Tardivon A, Margulis A, Mamelle G, et al. Value of high-frequency US for preoperative assessment of skin tumors. *Radiographics.* 1997; 17: 1559-1565
5. Gupta AK, Turnbull DH, Foster FS, Harasiewicz KA, Shum DT,

- Prussick R, et al. High frequency 40-MHz ultrasound. A possible noninvasive method for the assessment of the boundary of basal cell carcinoma. *Dermatol Surg.* 1996; 22: 131-136
6. Moore JV, Allan E. Pulsed ultrasound measurements of depth and regression of basal cell carcinoma after photodynamic therapy: relationship to probability of 1-year local control. *Br J Dermatol.* 2003; 149: 1035-1040
 7. Hoffmann K, Happe M, Schuller S, Stucker M, Wiesner M, Gottlober P, et al. Ranking of 20 MHz sonography of malignant melanoma and pigmented lesions in routine diagnosis. *Ultrasound Med.* 1999; 20: 104-109
 8. Ruocco E, Argentziano G, Pellacani G, Seidenari S. Noninvasive imaging of skin tumors. *Dermatol Surg.* 2004; 30: 301-310
 9. Hoffmann K, Stucker M, el-Gammal S, Altmeyer P. Digitale 20-MHz-sonographie des basalioms im b-scan. *Hautarzt.* 1990; 41: 333-339
 10. Fornage BD, McGavran MH, Duvic M, Waldron CA. Imaging of the skin with 20-MHz US. *Radiology.* 1993; 189: 69-76
 11. Harland CC, Bamber JC, Gusterson BA, Mortimer PS. High frequency, high resolution B-scan ultrasound in the assessment of skin tumours. *Br J Dermatol.* 1993; 128: 525-532
 12. Vaillant L, Grogard C, Machet L, Cochelin N, Callens A, Berson M. et al. High resolution ultrasound imaging: value in treatment of basocellular carcinoma by cryosurgery. *Annales de Dermatologie et de Venereologie.* 1998; 125: 500-504
 13. Walsh JS, Perniciaro C, Randle HW. Calcifying basal cell carcinomas. *Dermatol Surg.* 1999; 25: 49-51
 14. Bettencourt MS, Prieto VG, Shea CR. Trichoepithelioma: a 19-year clinicopathologic re-evaluation. *J Cutan Pathol.* 1999; 26: 398-404

Legends

Figure 1: Multiple hyper-sonographic spots in BCC (type A). Cotton flower-like spots with indistinct margins were scattered throughout the lesion.

Figure 2: Tissue specimen of Figure 1 (HE staining). Multiple foci of calcification were seen (black arrows).

Figure 3: Another case of BCC. The spots were smaller and brighter than those in Figure 1. Calcification foci were small and sparse in this case.

Figure 4: Clinical features of BCC on the cheek of a 73-year-old woman (A). This case was difficult to diagnose as BCC based on the dermoscopic findings (B). High-frequency sonography revealed hyper-sonographic spots in this lesion (C: white arrows), which strongly suggest a diagnosis of BCC. Pathologically, cornified cysts and clusters of parakeratotic cells were observed in the tumor nests (D).

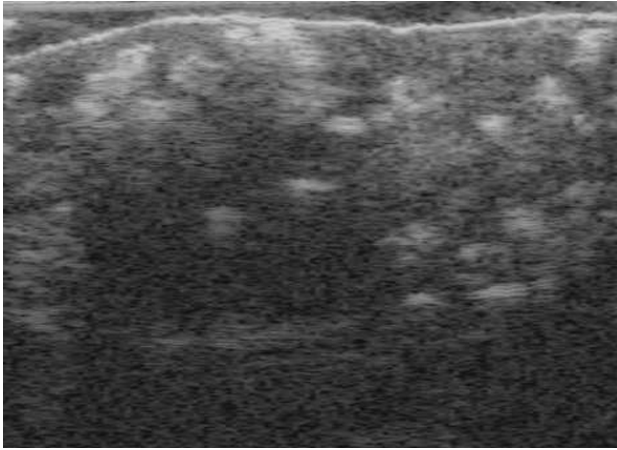


Figure 1

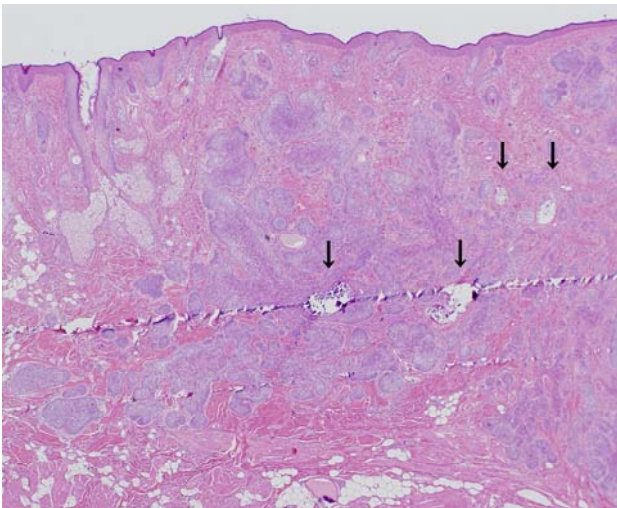


Figure 2

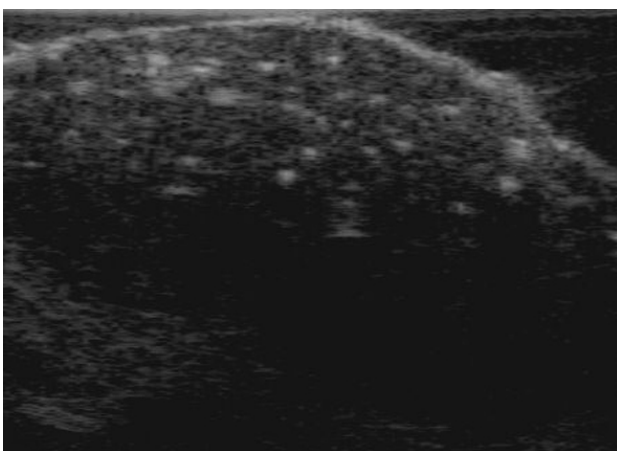


Figure 3



Figure 4(A)



Figure 4(B)

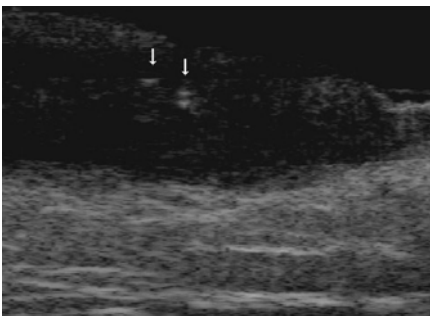


Figure 4(C)

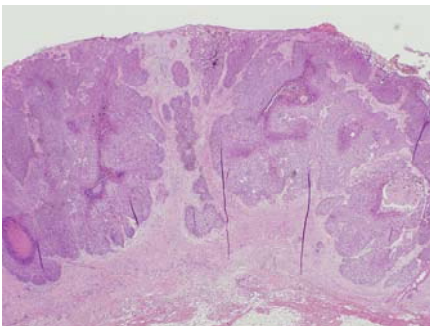


Figure 4(D)